Magnetotransport in anisotropic Pb films and monolayers

D. Lükermann, M. Gauch, M. Czubanowski, H. Pfnür, and C. Tegenkamp
Institut für Festkörperphysik, Leibniz Universität Hannover, Appelstrasse 2, D-30167 Hannover, Germany
(Received 26 November 2009; revised manuscript received 25 January 2010; published 24 March 2010)

The anisotropy induced by atomic steps of a Si(557) substrate in structure and magnetoconductance of ultrathin Pb films adsorbed on this surface is shown to be effectively shielded as a function of layer thickness, as found out by a combined study of low-energy electron diffraction and macroscopic four-point conductivity measurements as a function of Pb coverage, temperature, and magnetic field. In strong contrast to flat Si(111), substrate steps effectively compensate the lateral misfit (10%), leading to crystalline growth starting from the first monolayer. Multilayers already exceeding four physical monolayers (PML) form isotropic and percolated Pb islands even on this uniaxial surface. This structural anisotropy corresponds well to that found in dc conductivity measurements. As a function of temperature, strong localization effects with clear anisotropy become dominant for coverages below 4 PML. Strong anisotropic magnetotransport was found for Pb-wetting layers close to completion of the physical monolayer caused by an enhanced elastic scattering rate in the direction perpendicular to the step direction. While multilayers are characterized by weak localization, antilocalization is found for all monolayer structures due to strong spin-orbit coupling, which is effectively switched off around 1.3 ML (1 PML) below 78 K, where one-dimensional transport was seen along the step direction [C. Tegenkamp *et al.*, Phys. Rev. Lett. **95**, 176804 (2005)].

DOI: 10.1103/PhysRevB.81.125429 PACS number(s): 68.55.J−, 73.50.−h, 73.61.−r

I. INTRODUCTION

Metallic adlayers on semiconductor surfaces have been shown to be adequate model systems for highly correlated low-dimensional electron gases.[1–6] Making use of internal barrier structures at the interface, the substrate can be electronically decoupled. This opens the possibility to investigate electronic band structure, transport behavior, and correlate it with the structure of the film.[7] For instance, thin metallic films reveal quantum-well states (QWS) in spectroscopy, feeding back to the growth and modifying also the lateral conductance.[8–11]

By definition, only heteroepitaxial systems can be used for this approach. Thus interface effects such as metal-induced band-gap states, lattice mismatch, strain effects, etc., become inevitably important and affect the structural and electronic properties. For instance, favored heights (magic heights) of Pb islands by QWS effects depend sensitively on the substrate: whereas on Si(111) seven layer thick films are energetically favored,[12] growth of Pb on Si(111)-$\sqrt{3}\times 3$-Pb revealed five atomic layers,[13] while on graphene a magic height of four has been found.[8] Obviously, different interface effects lead to characteristic phase shifts, if the QWS are explained within the Bohr-Sommerfeld model.[14]

Although the influence of steps on equilibrium structures and growth have been extensively studied in the past,[15,16] only little is known about their indirect influence on other properties such as electronic transport. For many of these properties the typical spectroscopic tools such as electron spectroscopy have insufficient resolution to be helpful, with some exceptions, e.g., studies of in-plane QWS on vicinal metal surfaces.[17] On the contrary, surface transport provides clear step signatures, as shown below.

Surface transport measurements have become attractive in the last years,[7] triggered by the development of systems which allow spatially resolved four terminal conductivity [four-point probe (4PP)] measurements.[1,18] On the basis of the Drude model (in combination with spectroscopic data), the transport properties can be correlated with the carrier concentrations, density of states, and relaxation times. E.g., the type and concentration of defects leading to localization have been deduced from temperature-dependent conductivity measurements.[19,20] As model system for studies of the resistance of steps and to probe the anisotropy, metallic Ag$\sqrt{3}\times\sqrt{3}$ layers on Si(111) have been studied using 4PP techniques[21] and scanning tunneling potentiometry.[22] However, in order to be able to discriminate between different channels of electron scattering, magnetomeasurements are useful. This has been demonstrated at first for Pb/Si(111).[10]

In this paper Si(557) substrates were used with a step density around 20%. In order to interpret our transport data, the structure of monolayer and multilayer of Pb were analyzed by spot profile analysis-low-energy electron diffraction (SPA-LEED) and compared to previous results of Pb growth on Si(111).[23,24] We found strong anisotropy both in structure and transport, in particular, for monolayer coverages. Furthermore, directional-dependent transport measurements in combination with magnetic fields are performed. Thus, different scattering channels can be correlated with the uniaxial structure. Here we explicitly include spin-orbit scattering and demonstrate its importance in the monolayer regime. Particularly interesting is the uniaxial suppression of this scattering channel for coverages around 1.3 ML, which correlates with one-dimensional (1D) dc transport properties found at this coverage.[25,26]

II. EXPERIMENTAL SETUP

Low-doped Si(557) samples (15×15 mm^2 in size) with eight $TiSi_2$ contacts have been used to perform both LEED and four-point magnetoconductance and Hall measurements, both parallel and perpendicular to the wire-like structures

obtained by monolayer Pb films on vicinal Si(557). The contacts were fabricated by evaporation of Ti on the hydrofluoric acid (HF)-dipped samples in a vacuum of 10^{-6} mbar at elevated temperatures between 700 and 800 °C. Afterwards the samples were mounted on the sample holder and transferred into the main UHV chamber (base pressure 1×10^{-10} mbar). Crystalline Si surfaces were obtained by subsequent heating the samples by electron bombardment to temperatures of 1100 °C. The morphology was controlled in detail by SPA-LEED.

Pb was evaporated out of a ceramic crucible and the amount was controlled by a quartz microbalance. Pb films in the monolayer regime were produced in a two-step process by first depositing multilayers and subsequent heating to 640 K. This leaves behind a monolayer of Pb on the Si substrate and restructures the surface into (223) facets. A precise measurement of the residual coverage by SPA-LEED is obtained by using the Pb/Si(557) phase diagram reported elsewhere.[27] In order to vary the film thickness from this well-defined coverage, further minute amounts of Pb are evaporated onto the sample and monitored by the quartz microbalance. Alternatively, we also investigated multilayers of Pb that were prepared without high-temperature annealing steps. Under these conditions the (557) orientation remains stable. Here the films were postannealed to only 150 K to ensure good crystalline film quality. All coverages are given with respect to the atomic density on the silicon surface, i.e., for a physically closed monolayer (1 PML) film 1.3 ML are needed ($1\ \text{ML} = 7.83 \times 10^{14}\ \text{cm}^{-2}$).

For magnetotransport measurements the prepared Pb films are transferred *in situ* to the position of the magnet. The superconducting split coil magnet reaches magnetic fields of ± 4 T, which were directed perpendicular to the sample surface. Cooling of the samples during measurements was done by a cryostat with a temperature range of 4 K (with cooled radiation shield) to 300 K. The temperature is measured by a Si diode mounted on the cryostat itself and was calibrated using dummy samples with thermocouples.

III. RESULTS AND DISCUSSION

The intimate relationship between steps in heteroepitaxy and surface transport will be elucidated in the following. First the growth of Pb on Si(557) is briefly discussed and related to coverage-dependent transport regimes identified by variation in temperature. Finally, the peculiar electronic structure for the metallic Pb monolayer on Si(557) is emphasized by magneto transport measurements (Sec. III B).

A. Growth modes and transport regimes for Pb monolayer and multilayer

The adsorption of Pb on Si(557) leads to the formation of characteristic growth modes for monolayer and multilayer, which is reflected also by certain transport regimes. The growth modes are mediated by the Si(557) substrate itself but also the lattice misfit between Si and Pb has to be taken into account.

Si(557) has a miscut of 9.45° with respect to the (111) orientation. The steps run along the $[1\bar{1}0]$ direction and the

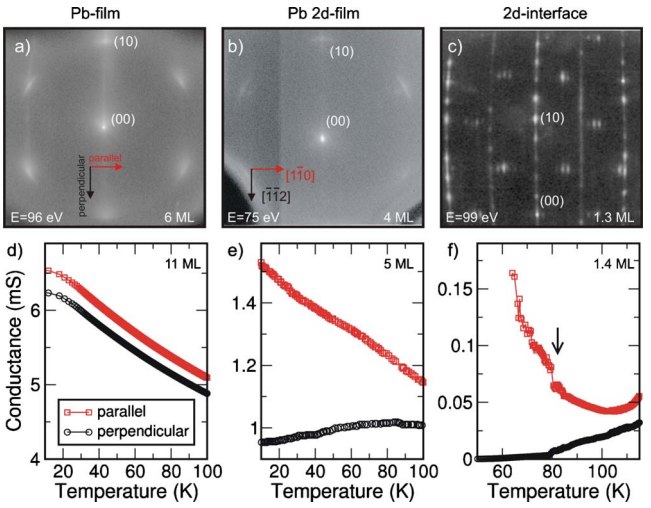

FIG. 1. (Color online) [(a)–(c)] LEED patterns and [(d)–(f)] temperature-dependent conductance measurements for three characteristic regimes: for coverages larger than 6 ML (4.5 PML) the transport is limited by the Pb film structure. A residual influence of the steps can be seen by the small anisotropy (left). 2D-film regime (middle): although the film structure is isotropic, for coverages up to 5 ML (≈4 PML) the transport through the film is strongly influenced by the anisotropy of the interface. The activated transport channel along the step train is caused by localization effects due to steps. 2D interface regime (right): The anisotropy both in structure and transport is further increased in the regime of Pb monolayer structures. Fur further details see text.

average terrace width is 5 2/3 atomic units. However, the step density is not homogeneous. Instead a periodic sequence of (112) and (111) facets is formed along the $[\bar{1}\bar{1}2]$ direction. On the (111) facets the characteristic (7×7) superstructure is formed. Further details about this surface can be found in Refs. 27–29.

Starting with thick Pb layers, i.e., ≥6 ML (which corresponds to about 4.5 PML, in the following the coverage is always given in ML, i.e., with respect to Si) the adsorption at low temperatures (10–50 K) followed by annealing to 150 K leads to the growth of a closed Pb film with (111) texture also on the (557) surface. Since high-temperature annealing cannot be performed here, contrary to the monolayer species (see below), the Si(557) step structure is conserved underneath. Exemplarily, the LEED pattern for 6 ML is shown in Fig. 1. The azimuthal broadening indicates the formation of rotational domains as a result of the lattice misfit of 8.8% between Pb and Si. This is in agreement with a previous SPA-LEED study, showing that the steps of the substrate are overgrown by larger Pb(111) crystallites if postannealing higher than 280 K is avoided.[30] From the full width at half maximum of radial scans through the first-order diffraction spots, domain sizes of around 10 nm are obtained. Compared to flat Si(111), where also rotation domains appear,[23] the domain sizes found for Pb/Si(557) are slightly larger, indicating a still small influence of steps in Pb epitaxy for thicker Pb films.

This small influence of steps is also reflected in the conductance of the films. The conductance was measured macroscopically with a modified van der Pauw geometry. This

enables us to measure the conductance both along the steps ($[1\bar{1}0]$ direction) and along the step train ($[\bar{1}\bar{1}2]$ direction). E.g., for a 10 ML film ($\approx$8 physical Pb layers) the conductance is on the order of 5 mS and can be well discriminated from possible parasitic surface and interface contributions. The conductance of the clean substrate is below 1 μS below 150 K. Figure 1(d) shows the conductance of a 11 ML film in the temperature range between 20–100 K. As expected for a metallic film, the conductance decreases with increasing temperature due to electron-phonon scattering. Furthermore, the conductance measured across the steps is lower by approximately 5%. For this film thickness, d_{film}, the mean-free path of the electrons is still less than d_{film} (see below), and the anisotropy of the Pb-Si interface is transferred into the Pb film causing the slight anisotropy in transport.

A different transport scenario becomes visible in the low-coverage multilayer regime [two-dimensional (2D) film]. Although the films appear to be isotropic in structure for coverages between 3 and 5 ML [cf. with Fig. 1(b)], the transport is strongly influenced by the Pb-Si interface. E.g., at 5 ML metallic transport behavior was found only along the steps while in the direction across the steps the conductance increases with increasing temperature.[26] Obviously, the high step concentration of almost 20% leads to (strong) localization effects. Furthermore, as the film thickness is reduced by a factor of 2, the absolute value of the conductance (along the steps) decreases by a factor of 5. Together with the increase in the anisotropy in conductance, this directly demonstrates the importance of steps. The critical film thickness of 5 ML (4 PML) for the change in general transport behavior coincides closely with the Fermi wavelength deduced from the QWS behavior seen with spectroscopy for Pb(111) islands on Si(111). (λ_F=10.6 Å, Ref. 31). Since there are multiple crossings of the Fermi level at this layer thickness,[32] the value for λ_F should be taken as a weighted average. Obviously, the propagating electrons scatter effectively and directly at potentials stemming from step sites. The crossover between both bulk and interface dominated transport in Pb films is fully supported by results measuring the change in conductance during evaporation of Pb.[33]

Extremely anisotropic metallic films are only obtained for Pb wetting layers on Si(557). Both the local facet structure and the reconstruction on the (111) mini terraces can be tuned by the Pb coverage as revealed by SPA-LEED.[27,34,35] In brief, the adsorption of Pb and subsequent annealing to 640 K leads to destabilization of the original (557) surface. The annealing at this point is important in order to have a percolated metallic structure. Otherwise, if the (7×7) reconstruction of the Si substrate is not destroyed, the Pb nucleates into nonpercolated islands. By increasing gradually the coverage from 1.2 to 1.6 ML (112)-, (335)-, (223)-, and a metastable (557)-facet are formed. Along the step direction, various Pb reconstructions were identified varying from $\sqrt{7}\times\sqrt{3}$ below 1.3 ML to $\sqrt{3}\times\sqrt{3}$ phases with domain walls (so-called linear phases) above this coverage.[24,36,37]

Only Pb chain structures obtained after deposition of 1.31 ML and annealing to 640 K [Fig. 1(c)] represent a realization of extremely anisotropic quasi-one-dimensional transport:[25,38] below 78 K the conductance in the direction perpendicular to the steps is almost zero. This insulating state is caused by perfect Fermi nesting. Along the steps, on the contrary, conductance of a delocalized electron gas was found due to split-off bands crossing the Fermi surface. Above 78 K a refaceting phase transition switches the system back into a 2D state, where activated transport is found in both directions.[34] For our macrosopic four-point probe method, the sharpness of this phase transition in conductance depends crucially on the perfectness of the (223) facet structure on a mesoscopic scale and on the exact coverage (band filling). For the example shown in Fig. 1(f) both the coverage was higher but also the substrate before adsorption was slightly facetted, most likely due to stress during mounting the Si sample. Nonetheless, the phase transition is still visible (arrow). Since we will concentrate here particularly on the anisotropic conductance in 2D systems, this imperfection will not affect our conclusions obtained from magnetotransport measurements.

B. Magnetotransport measurements: Strong spin-orbit coupling in monolayer structures

As we have shown above, Pb films exhibit significant conductance, which, depending on the conditions of preparation and layer thickness, is partly thermally activated and partly metallic. For annealed films in the monolayer range it can even be thermally switched. On these effects of partly strong localization, characterized by thermal activation of free charge carries, those of weak localization (WL) of these free carriers are superimposed. They are caused by scattering at defects within the layers and at the interfaces. Scattering of free carriers and weak localization can be studied by applying a strong magnetic field at constant temperature in studies of electronic transport.

This is the type of measurements we will concentrate on in this section. As we will show, there is a fundamental difference in magnetotransport in Pb films and monolayer structures, characterized by strong spin-orbit coupling. Scattering of electrons can be either elastic with a characteristic average time between two scattering events, τ_o, inelastic (τ_i), or it may be due to spin-orbit scattering (τ_{so}).

WL is influenced by these scattering times in a characteristic way. In case that the elastic scattering rate $1/\tau_o$ is higher than the inelastic rate $1/\tau_i$, interference effects between electrons contribute to the total resistance. Although in general the phases of adjacent trajectories are uncorrelated, the condition of backscattering is still well defined, and partial waves elastically backscattered along various scattering paths can interfere constructively, giving rise to WL. An externally applied magnetic field can lift this constructive inference. Thus, a reduction in resistance is expected in presence of a magnetic field [negative magnetoresistance (MR)].[39]

Indeed, WL was found for Pb multilayers on Si(557) (Fig. 2), if the temperature is not too close to T_c of superconductivity for the Pb films. Otherwise superconducting contributions are dominant turning the negative into a positive MR.[40,41] The importance of the latter effect has been demonstrated for Pb films on Si(111) measured at 7 K.[10] Although

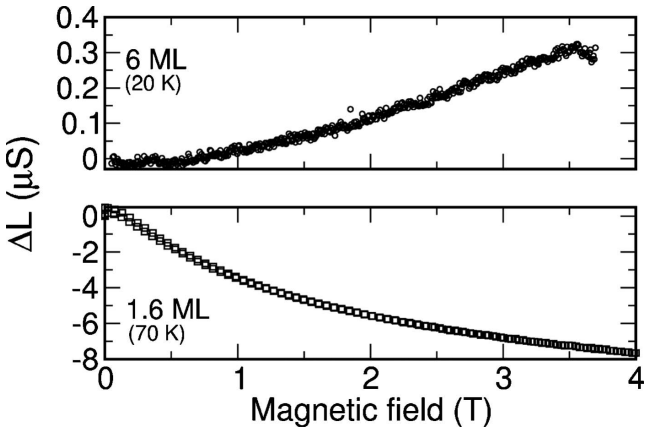

FIG. 2. Magnetoconductivity ΔL of Pb/Si(557) for different film thickness (along the $[1\bar{1}0]$ direction perpendicular to the steps). While for thick layers WL is found, the monolayer reveals a WAL behavior, pointing toward a strong spin-orbit coupling. The conductances at zero magnetic field were 5 mS and 1 mS for the 6 ML and 1.6 ML film, respectively.

spin-orbit coupling must be considered in order to describe the electronic band structure accurately,[8] in transport only states within k_BT around the Fermi energy are contributing. angle resolved photoemission spectroscopy (ARPES) has revealed that these states are rather similar to those of a free electron gas, hence, antilocalization effects are not expected for Pb films.

For Pb monolayers on Si(557), exemplarily shown for 1.6 ML in Fig. 2, the situation is reversed and a positive MR has been found. Since the data were taken at 70 K, superconductivity fluctuations can be safely ruled out here. As we will show below the WL is turned into a weak antilocalization (WAL) regime because spin-orbit scattering (τ_{so}) is dominant and of the same order as τ_o. In this case the 4π invariance of the spin-wave function changes the constructive interference into a destructive interference.[39] Indeed, it has been shown recently by ARPES that large Rashba spin splitting is dominant in metallic monolayers of Bi grown on semiconducting substrates.[42,43] Apart from the different mechanisms of interference in multilayer and monolayer also the magnitude of the effect is significantly different. While for multilayers the effect of weak localization is on the order of $10^{-4}-10^{-5}$, we found that it is larger by typically 2 orders of magnitude in 2D systems.

A quantitative description of spin-orbit interaction and MR in two-dimensional systems was elaborated by Hikami *et al.*[44] The change in the magnetoconductance $\Delta L=L(B)-L(0)$ is given by $\Delta L(B)=-L_{00}[f(\frac{B_o+B_{so}}{B})-\frac{3}{2}f(\frac{4/3B_{so}+B_i}{B})+\frac{1}{2}f(\frac{B_i}{B})]$ with $f(B_\nu/B)=\Psi(1/2+B_\nu/B)-\ln(B_\nu/B)$, where Ψ is the digamma function and $L_{00}=e^2/(2\pi^2\hbar)$. B denotes the externally applied magnetic field and the B_ν, $\nu=i,o,so$ are defined as $B_\nu=\hbar\cdot n/(4ev_F^2\tau_o\tau_\nu)$. Hence, for a given Fermi velocity v_F of the electrons with charge e in an n-dimensional system all essential scattering parameters τ_i (inelastic), τ_o (elastic), and τ_{so} (spin orbit) can be determined. Within this formalism influences of magnetic impurities are neglected as well as Coulomb interaction effects.

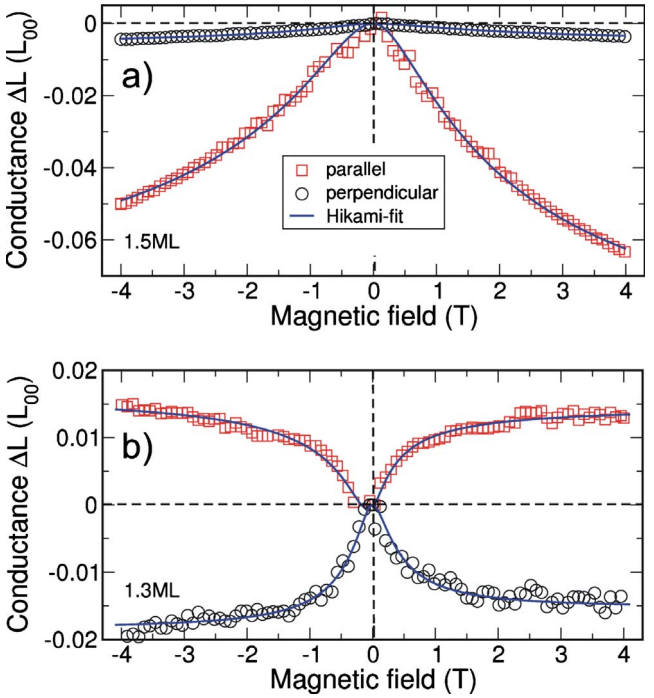

FIG. 3. (Color online) (a) Magnetoconductance of 1.5 ML/Si(557) measured at 40 K along (squares) and perpendicular (circles) to the step direction: The zero-magnetic conductances are $L_\perp=0.03$ mS and $L_\parallel=0.18$ mS for the perpendicular and parallel direction, respectively. (b) Corresponding curves for 1.3 ML coverage (50 K). The magnetotransport measured along the steps has switched from positive to a negative MR. The solid lines represent results from a Hikami analysis.

Figure 3(a) shows the magnetoconductance measured at 40 K for 1.5 ML of Pb along and across the step direction with WAL in both directions. According to the results presented above, the transport was found to be strongly anisotropic in this coverage regime. In this particular case the conductance at zero-magnetic field along the steps was around six times larger than across the step direction ($L_\parallel/L_\perp=6.$). The solid lines represent best fits according to the Hikami formalism. The characteristic time constants averaged over many measurements are summarized in Table I together with those obtained previously for Pb/Si(111).[11]

The experiments have been performed at temperatures between 40–50 K in order to rule out superconducting effects. Thus, compared to data obtained from the Pb/Si(111) system,[11] τ_i is smaller by 2 orders of magnitude. However, since the variation in temperature affects only the inelastic time constant, the difference in the values of τ_o and τ_{so} are related to different growth modes and the step structure, but also to changes in the band structures as a function of layer thickness. Compared to multilayer structures of Pb, τ_o is increased, while τ_{so} is significantly decreased for the Pb monolayer structures grown on Si(557). Both the elastic and the spin-orbit scattering rates are dominant and of the same order of magnitude. Thus, WAL is expected according to the model of the rotating spin described above. In contrast, the spin-orbit scattering rate for multilayers was found to be 2 orders of magnitude lower.

TABLE I. Inelastic (τ_i), elastic (τ_o), and spin-orbit (τ_{so}) scattering times for Pb films and monolayers grown on Si(111) and Si(557) measured along ($\parallel$) and across ($\perp$) the step direction. The data for Pb/Si(111) were taken from Ref. 10. The scattering times for ≈1 ML/Si(557) are averaged values obtained for coverages between 1.2 and 1.5 ML including the 1.3 ML regime, where WL has been found along the steps. For details see text.

	6 ML		≈1 ML		
	Si(111)	Si(557)	Si(111)	Si(557)-$\parallel$	Si(557)-$\perp$
T (K)	7	15	7	40	40
τ_i (s)	2×10^{-12}	2×10^{-14}	2×10^{-12}	2×10^{-14}	2×10^{-14}
τ_o (s)	3×10^{-16}	5×10^{-15}	1×10^{-16}	2×10^{-14}	5×10^{-15}
τ_{so} (s)	2×10^{-10}	1×10^{-13}	5×10^{-11}	6×10^{-13}	3×10^{-14}

Furthermore, as expected for anisotropic transport, the elastic and the spin-orbit scattering rate are slightly higher on average in the direction of the step train compared to the perpendicular direction. Here the ratio of the elastic scattering times $\tau_{o,\parallel}/\tau_{o,\perp}=4$ is in good agreement with the anisotropy in conductance, i.e., the elastic scattering rates are essentially controlled by the steps.

Taking the Fermi velocity in the $[\bar{1}\bar{1}2]$ direction of 5×10^5 m/s from spectroscopy,[38] we find an average elastic mean-free path $l=v_F\cdot\tau_{o,\perp}$ of 2.5 nm in reasonable agreement with the average step spacing of 1.9 nm for a (557)-orientated surface. For $\tau_{o,\perp}$ an average value of 5×10^{-15} s was used. The variation in τ_o as a function of coverage is shown in detail in Fig. 4(a). For the whole monolayer coverage regime the parallel component is higher than $\tau_{o,\perp}$. While the scatter of the data is comparably small along the step direction, the values taken from conductance measurements across the step direction scatter by 1 order of magnitude. This is most likely caused by imperfect ordering of the step structure and its variation by different layer preparations.

The peculiar transport behavior below 80 K of the perfectly ordered Pb-chain structure after deposition of 1.3 ML has been emphasized above. A special signature is also seen in magnetotransport measurements [see Fig. 3(b)] at this Pb concentration. While in the perpendicular direction WAL is seen, similar to the situation at 1.5 ML, the magnetoconductance is reversed for the parallel direction. From the Hikami analysis we derive a spin-orbit scattering time, which around the Pb concentration of 1.3 ML is larger by 3 orders of magnitude than outside this coverage range. The results of τ_{so} for both directions are plotted in Fig. 4(b). Contrary to the behavior of τ_o, spin-orbit scattering seems to be sensitive predominantly in the direction along the wires.

At this moment, we can only give a tentative explanation for this effect, which relies on (spin-averaged) spectroscopic data from ARPES (Ref. 38) at a Pb concentration of 1.3 ML and on our studies of long-range order[35] in the step decoration at Pb coverages up to 1.5 ML, coupled with first conductance data at these Pb concentrations. As shown in Ref. 38, the nested Fermi surface at 1.3 ML consists of characteristic points that are separated in momentum space by $k_\perp=2\pi/d$, which results in band filling in the direction normal to the steps and opening of a band gap in this direction. In other words, a one-dimensional Peierls transition takes place at 78 K, resulting in insulating behavior normal, but metallic properties along the Pb-covered terraces. In the momentum direction parallel to the steps ($k_\parallel$) there are two series of Fermi points from split bands, possibly induced also by spin-orbit coupling. One forms a fundamental gap of approximately 20 meV (Ref. 38) so that also at a temperature of 50 K its contribution to conductance is strongly suppressed compared to the second band that is mainly responsible for the observed 1D conductivity. If these bands are spin polarized, it is obvious that scattering of electrons close to the Fermi level from $+k_\parallel$ to $-k_\parallel$ does not allow spin umklapp. This results in effective suppression of spin-orbit scattering under these conditions.

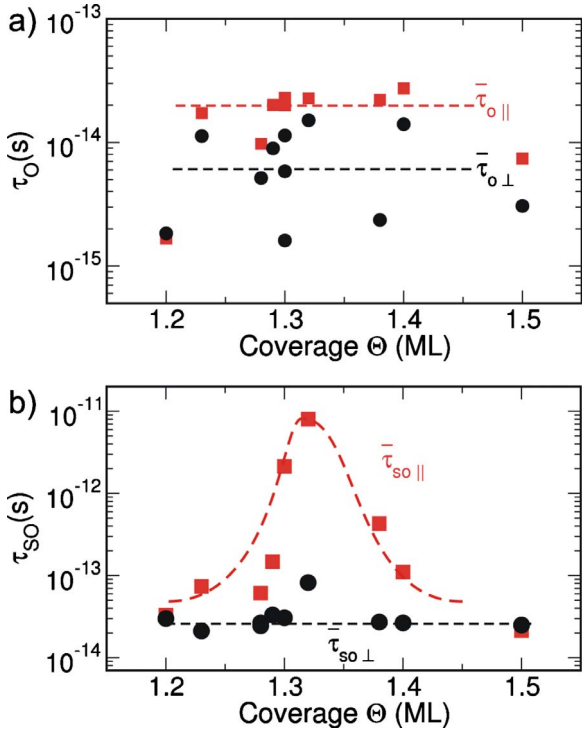

FIG. 4. (Color online) (a) Elastic scattering time τ_o and (b) spin-orbit scattering time τ_{so} as derived from the Hikami analysis of magnetoconductance curves for different Pb coverages (T=40–50 K). The dashed lines are guides to the eye.

The 1D Peierls insulator still exists when the Pb coverage is increased up to 1.5 ML (Ref. 35) since the added coverage decorates the steps with Pb chains whose separation is again long-range ordered. According to our model, this results again in new subbands that are completely filled in $\perp$ direction, but with a continuously shrinking band gap in this direction as a function of excess Pb concentration. At finite measuring temperatures-our measurements were carried out at 50 K, as mentioned above-a reduction in the size of the band gap as a function of Pb concentration leads to a more and more isotropic conductance, in agreement with our data.[33] At the same time, this lifts the suppression of spin-orbit scattering gradually as a function of Pb concentration, as observed here.

IV. SUMMARY AND OUTLOOK

In summary, we have presented transport results of Pb multilayers and monolayers grown on Si(557). In particular, the influence of steps has been elucidated by systematic variation in Pb coverage, temperature, and external magnetic fields. As seen by SPA-LEED and transport measurements, steps effectively compensate the stress within this heteroepitaxial system with its large lattice mismatch, so that closed layers are formed and above a thickness of five physical layers only a small anisotropy remains both in structure and in conductance.

Anisotropy for thinner layers also appears as anisotropic elastic and spin-orbit scattering times in magnetotransport. Compared to results obtained for multilayers, the spin-orbit scattering time is significantly reduced for closely packed Pb monolayer structures on Si(557). This shows that the electronic states near the Fermi energy are modified by spin-orbit coupling.

Although experimentally demanding, magnetotransport measurements of the 1D transport phase below 78 K were successfully carried out. The reduced spin-orbit scattering rate found in this study for 1.3 ML at low temperatures can be taken as a hint toward uniaxially extended states along the steps, which may be spin split.[38] In any case, this finding seems to be closely related to the formation of (223) facets and corresponding one-dimensional band filling. Interestingly, this phenomenon is not washed out by the presence of larger (111) terraces or local facet orientations that differ from (223), which is necessary in order to maintain the macroscopic surface orientation. This means that their contribution is sufficiently small. Nonetheless, further high-resolution (spin-polarized) measurements are needed. Unfortunately, the inelastic scattering is dominating above the phase transition temperature, so that magnetotransport measurements revealing eventually different spin-orbit scattering times above the phase transition temperature will be extremely difficult to measure.

ACKNOWLEDGMENT

Financial support by the Deutsche Forschungsgemeinschaft is gratefully acknowledged.

[1] T. Kanagawa, R. Hobara, I. Matsuda, T. Tanikawa, A. Natori, and S. Hasegawa, Phys. Rev. Lett. **91**, 036805 (2003).
[2] J. N. Crain, A. Kirakosian, K. N. Altmann, C. Bromberger, S. C. Erwin, J. L. McChesney, J. L. Lin, and F. J. Himpsel, Phys. Rev. Lett. **90**, 176805 (2003).
[3] H. W. Yeom, S. Takeda, E. Rotenberg, I. Matsuda, K. Horikoshi, J. Schäfer, C. M. Lee, S. D. Kevan, T. Ohta, T. Nagao, and S. Hasegawa, Phys. Rev. Lett. **82**, 4898 (1999).
[4] J. R. Ahn, P. G. Kang, K. D. Ryang, and H. W. Yeom, Phys. Rev. Lett. **95**, 196402 (2005).
[5] T. Tanikawa, I. Matsuda, T. Kanagawa, and S. Hasegawa, Phys. Rev. Lett. **93**, 016801 (2004).
[6] C. Brun, I.-Po Hong, F. Patthey, I. Yu. Sklyadneva, R. Heid, P. M. Echenique, K. P. Bohnen, E. V. Chulkov, and W. D. Schneider, Phys. Rev. Lett. **102**, 207002 (2009).
[7] P. Hofmann and J. W. Wells, J. Phys.: Condens. Matter **21**, 013003 (2009).
[8] J. H. Dil, T. U. Kampen, B. Hülsen, T. Seyller, and K. Horn, Phys. Rev. B **75**, 161401(R) (2007).
[9] J. H. Dil, F. Meier, J. Lobo-Checa, L. Patthey, G. Bihlmayer, and J. Osterwalder, Phys. Rev. Lett. **101**, 266802 (2008).
[10] O. Pfennigstorf, A. Petkova, H. L. Guenter, and M. Henzler, Phys. Rev. B **65**, 045412 (2002).
[11] O. Pfennigstorf, A. Petkova, Z. Kallassy, and M. Henzler, Eur. Phys. J. B **30**, 111 (2002).
[12] K. Budde, E. Abram, V. Yeh, and M. C. Tringides, Phys. Rev. B **61**, R10602 (2000).
[13] N. Miyata, K. Horikoshi, T. Hirahara, S. Hasegawa, C. M. Wei, and I. Matsuda, Phys. Rev. B **78**, 245405 (2008).
[14] M. Milun, P. Pervan, and D. P. Woodruff, Rep. Prog. Phys. **65**, 99 (2002).
[15] H. C. Jeong and E. D. Williams, Surf. Sci. Rep. **34**, 171 (1999).
[16] C. Tegenkamp, J. Phys.: Condens. Matter **21**, 013002 (2009).
[17] C. Didiot, Y. Fagot-Revurat, S. Pons, B. Kierren, C. Chatelain, and D. Malterre, Phys. Rev. B **74**, 081404(R) (2006).
[18] S. Hasegawa, I. Shiraki, F. Tanabe, R. Hobara, T. Kanagawa, T. Tanikawa, I. Matsuda, C. L. Petersen, T. M. Hansen, P. Boggild, and F. Grey, Surf. Rev. Lett. **10**, 963 (2003).
[19] S. Yamazaki, I. Matsuda, H. Okino, H. Morikawa, and S. Hasegawa, Phys. Rev. B **79**, 085317 (2009).
[20] C. Liu, I. Matsuda, S. Yoshimoto, T. Kanagawa, and S. Hasegawa, Phys. Rev. B **78**, 035326 (2008).
[21] I. Matsuda, M. Ueno, T. Hirahara, R. Hobara, H. Morikawa, C. Liu, and S. Hasegawa, Phys. Rev. Lett. **93**, 236801 (2004).
[22] J. Homoth, M. Wenderoth, T. Druga, L. Winking, R. G. Ulbrich, C. A. Bobisch, B. Weyers, A. Bannani, E. Zubkov, A. M. Bernhart, M. R. Kaspers, and R. Möller, Nano Lett. **9**, 1588 (2009).
[23] A. Petkova, J. Wollschläger, H.-L. Günter, and M. Henzler, Surf. Sci. **482-485**, 922 (2001).
[24] A. Petkova, J. Wollschläger, H.-L. Günter, and M. Henzler, Surf. Sci. **471**, 11 (2001).
[25] C. Tegenkamp, Z. Kallassy, H. Pfnür, H.-L. Günter, V. Zielasek,

and M. Henzler, Phys. Rev. Lett. **95**, 176804 (2005).
[26] C. Tegenkamp, Z. Kallassy, H.-L. Günter, V. Zielasek, and H. Pfnür, Eur. Phys. J. B **43**, 557 (2005).
[27] M. Czubanowski, A. Schuster, S. Akbari, H. Pfnür, and C. Tegenkamp, New J. Phys. **9**, 338 (2007).
[28] D. H. Oh, M. K. Kim, J. H. Nam, I. Song, C. Y. Park, S. H. Woo, H. N. Hwang, C. C. Hwang, and J. R. Ahn, Phys. Rev. B **77**, 155430 (2008).
[29] R. Zhachuk and S. Pereira, Phys. Rev. B **79**, 077401 (2009).
[30] E. Hoque, A. Petkova, and M. Henzler, Surf. Sci. **515**, 312 (2002).
[31] Y.-F. Zhang, J.-F. Jia, T.-Z. Han, Z. Tang, Q.-T. Shen, Y. Guo, Z. Q. Qiu, and Q.-K. Xue, Phys. Rev. Lett. **95**, 096802 (2005).
[32] I. Vilfan and H. Pfnür, Eur. Phys. J. B **36**, 281 (2003).
[33] D. Lükermann, H. Pfnür, and C. Tegenkamp (unpublished).
[34] M. Czubanowski, A. Schuster, H. Pfnür, and C. Tegenkamp, Phys. Rev. B **77**, 174108 (2008).
[35] M. Czubanowski, H. Pfnür, and C. Tegenkamp, Surf. Sci. **603**, L121 (2009).
[36] M. Yakes, V. Yeh, M. Hupalo, and M. C. Tringides, Phys. Rev. B **69**, 224103 (2004).
[37] S. Stepanovsky, M. Yakes, V. Yeh, M. Hupalo, and M. C. Tringides, Surf. Sci. **600**, 1417 (2006).
[38] C. Tegenkamp, T. Ohta, J. L. McChesney, H. Dil, E. Rotenberg, H. Pfnür, and K. Horn, Phys. Rev. Lett. **100**, 076802 (2008).
[39] G. Bergmann, Phys. Rep. **107**, 1 (1984).
[40] K. Maki, Prog. Theor. Phys. **40**, 193 (1968).
[41] R. S. Thompson, Phys. Rev. B **1**, 327 (1970).
[42] I. Gierz, T. Suzuki, E. Frantzeskakis, S. Pons, S. Ostanin, A. Ernst, J. Henk, M. Grioni, K. Kern, and C. R. Ast, Phys. Rev. Lett. **103**, 046803 (2009).
[43] S. Hatta, T. Aruga, Y. Ohtsubo, and H. Okuyama, Phys. Rev. B **80**, 113309 (2009).
[44] S. Hikami, A. I. Larkin, and Y. Nagaoka, Prog. Theor. Phys. **63**, 707 (1980).